JNRD
JOURNAL OF NATURAL RESOURCES AND DEVELOPMENT

JOURNAL OF NATURAL RESOURCES AND DEVELOPMENT

Research article

Evaluation of the water supply potential of nature-based and reservoir-based drought adaptation measures under climate change scenarios for a rural catchment in South-east Brazil

Ley, Alexander[1,3]; McNamara, Ian[2]; Nauditt, Alexandra[2]; Mohn, Rainer[3]

[1] Jade University of Applied Science Wilhelmshaven/Oldenburg/Elsfleth, Ofener Straße 16/19, 26121 Oldenburg, Germany
[2] Institute for Technology and Resources Management in the Tropics and Subtropics (ITT), Technical University of Applied Science Cologne, Betzdorfer Strasse 2, 50679 Cologne, Germany
[3] IWARU Institute for Infrastructure, Water, Resources, Environment, University of Applied Science Münster, Corrensstraße 25, 48149 Münster, Germany
Corresponding author: Alexander Ley, E-Mail: alexander.ley@jade-hs.de

Article history

Received 28.04.2021
Accepted 10.02.2022
Published 10.06.2022

Keywords

Drought
WEAP
Climate Change
RCP 2.6
RCP 8.5
Silvopasture
Nature-based solutions
Brazil

Abstract

Tropical rural and unregulated catchments are often affected by droughts due their lack of storage capacity and dependence on rainfed agricultural production. In 2014/2015, the Muriaé catchment in South-East Brazil suffered severe drought impacts. In this study, we evaluated the effect of expected climatic changes and two contrasting adaptation measures on streamflow; one measure representing conventional grey infrastructure and the other a nature-based solution. We used the Water Evaluation and Planning System (WEAP) tool to assess changes in streamflow when increasing reservoir storage and implementing basinwide silvopasture. These intervention scenarios were combined with regional climate change projections for the RCP 2.6 (low) and 8.5 (high) emission scenarios. The results showed higher precipitation and lower temperatures for the 2.6 scenario compared to the historical period (2000 – 2018). Yet, for the RCP 8.5 scenario, dry season flow (JJA) was expected to decrease by an average of 42% compared to the historical period. Adding the adaptation measures, simulations suggested that the modelled reservoir volume was sufficient to maintain the 90th percentile flow (Q90) during most of the modelled drought periods. Furthermore, our results showed that the implementation of silvopasture alone would increase streamflow at the catchment outlet by a maximum of 4%. In addition, it would decrease streamflow peaks during the wet season by a maximum of 4%. We conclude that our approach of applying climate projections and potential land use and storage scenarios to water allocation modelling can deliver valuable decision support to water resources managers and regional planners.

1. Introduction

Seasonal meteorological droughts and hydrological droughts are recurrent phenomena, even in tropical regions (Nauditt et al., 2017b) and are expected to become more frequent and intense in the future (Ortiz, 2012; Trenberth et al., 2014; Erfanian et al., 2017). The majority of drought hazard monitoring and management measures have been implemented in arid and semi-arid regions (UN-ISDR, 2005). In contrast, coping with droughts in tropical regions has gained significantly less interest in science and water management (UN-ISDR, 2009; UNDP, 2011). Rural and unregulated tropical catchments tend to be extremely vulnerable to meteorological droughts, due to their lack of storage capacity and key economic activities such as rainfed agriculture and livestock production that solely depend on rainfall (Nauditt et al., 2019a, 2020).

Climate change is expected to impact drought frequency, duration and severity patterns in South America (Erfanian et al., 2017). Marengo et al. (2012) predicted lower mean annual precipitation (-6%) and increased mean temperature (+ 1.7 °C) over Brazil by 2040. Avila-Diaz et al. (2020) concluded that there will be an increase in intensity and frequency of extreme weather events in Brazil with rising temperature indices such as annual maximum and minimum temperature varying between 1.4 to 2.3 °C under the Representative Concentration Pathway (RCP) 4.5 and 1.9 to 3.1 °C under RCP 8.5. Drought intensity and severity, derived through indices such as Standardized Precipitation Index (SPI) and Standardized Precipitation-Evaporation Index (SPEI), are expected to rise by the end of the century (Spinoni et al., 2020). Focusing on the South-East region of Brazil, projections indicate intense warming during the summer season with maximum temperatures reaching approximately +8 °C above normal during 2070 – 2100 (RCP 8.5) and precipitation is strongly reduced during summer, possibly affecting reservoirs and water supply in the region (Lyra et al., 2018).

Drought situations have significant socio-economic impacts on water-dependent sectors and can affect large areas (Maia et al., 2015). For this reason, studies on the impact of climate change and suitable adaptation of water resources in river basins has gained increasing scientific concern (e.g. Chebet et al., 2019; Sridharan et al., 2019).

Two common strategies for drought adaptation are grey infrastructure and nature-based solutions (NBS). NBS for water are inspired by natural designs and ecosystem services to contribute to sustainable water management with benefits that are similar to conventional grey (built/physical) water infrastructure (UNESCO and World Water Assessment Programme, 2018). Agroforestry can be considered a NBS that has the potential to limit the effect of droughts (Keesstra et al., 2018) and reverse soil degradation (Dias-Filho, 2014). Silvopastoral systems (SPS) are a type of agroforestry with livestock production as the main target. In SPS, the animals graze directly under trees, where vegetation is either natural or planted (Nahed-Toral et al., 2013). Trees in pasture reduce runoff, thereby improving hydrological services of the landscape (Benegas et al., 2014) and also have the potential to improve animal production performance in tropical regions (de Oliveira et al., 2014). Furthermore, when planted with an intermediate surface coverage, trees in pasture promote infiltration (Ilstedt et al., 2016).

When planning interventions for drought management in a catchment, water allocation models are useful tools in decision making for planners. Such models of the socio-hydrological system can be implemented to quantify both seasonal and long-term deficits between system supply and demands and for different scenarios including interventions such as introducing dam storage capacity, changing irrigation coverage, and hydro-economic modelling (e.g. Alamanos et al., 2019; McNamara et al., 2020). To address potential climatic changes in such socio-hydrological analyses, modellers can use climate projections from downscaled global climate models (Fowler et al., 2007) or artificial projections indicating future escalation of climate extremes as droughts.

DOI: 10.18716/ojs/jnrd/2022.12.02

In the context of the challenges described above, the overall objective of this work is to recommend suitable drought adaptation measures for unregulated tropical catchments, based on the example of the Muriaé basin in South-East Brazil. The specific objectives of this study are to: i) characterise historical long term hydro-climatic patterns in the catchment to determine calibration and validation periods corresponding to both wet and dry periods; ii) provide water availability and demand scenarios for the Muriaé basin, reflecting climate change projections and socio-economic development; and iii) estimate and compare the effects of potential adaptation measures (infrastructure and nature-based) on future water availability in the basin.

2. Data and Methodology

2.1 Study area

The Muriaé catchment in South-East Brazil is a typical example for a vulnerable unregulated tropical catchment, similar to many others in the region and worldwide (Nauditt et al., 2020).

The Muriaé basin is located in the South-East region of Brazil; it covers an area of 8,292 km² and extends over the borders of the Federal States Minas Gerais and Rio de Janeiro. The Rio Muriaé is the last important tributary on the left bank of the main river Paraíba do Sul before it flows into the Atlantic Ocean. The area is inhabited by about 330,000 people, and Muriaé, Carangola and Itaperuna are the biggest cities and industrial centres. A strongly seasonal tropical savanna climate characterises the catchment (Peel et al., 2007) with a high elevation gradient from 10 to 1,900 meters above sea level.

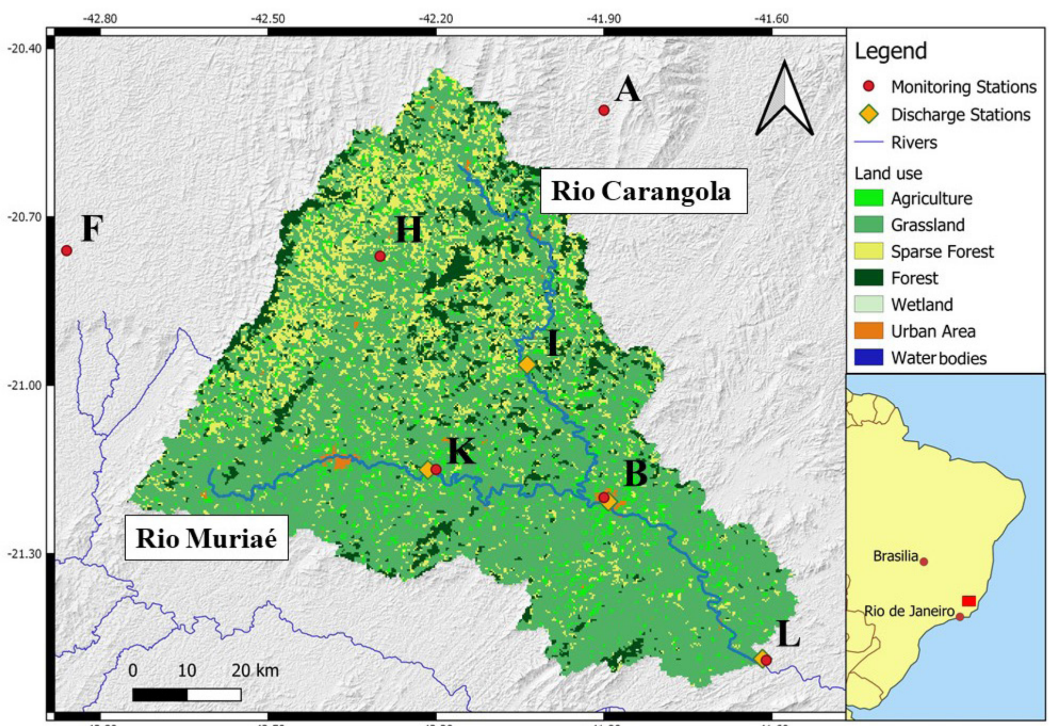

Figure 1: Map of the Muriaé catchment, the land use, its location in Brazil, and six out of the eleven climate stations used to derive estimates for precipitation, sunshine-hours, temperature, humidity and wind speed – denotations are explained in Table 1

The geology of basin is dominated by granites and gneisses associated with the formation of the Ribeira Belt, but also includes orthogranulites, meta-sedimentary and metavolcanic-sedimentary rocks. Punctual granitoids and loose sediments are present in the lower floodplain. These underground features lead to high permeability, high groundwater recharge rates and reduced streamflow reaching the downstream river system compared to catchments with low permeability, resulting in a higher hydrological drought risk than the upstream region (Nauditt et al., 2020).

Land use in the basin has undergone significant change: in the 18th century sugar cane and coffee were the most common crops, with coffee production growing until the 20th century, when intensive cattle farming and milk production substituted most agricultural uses (Carvalho and Torres, 2002). These land use changes from coffee production to pasture planes exposed soil to severe water erosion (Le Breton, 2000). Nowadays, rainfed horticulture is dominant in the upstream area located in the state Minas Gerais (Nauditt et al., 2020), while livestock and milk production is the main economic activity in the downstream region of Italva (Fischer et al., 2018). In 2018, 68% of the Muriaé catchment area was classified as grassland and pasture plains (ESA, 2019) (Figure 1), offering potential for adaptive land use change towards SPS (Fischer et al., 2018).

2.2 Data

Hydro-climatic and streamflow data

Data from eleven hydro-climatic measurement stations were analysed to characterise hydro-climatic conditions in the basin (Table 1). Five of the stations are located in the study area, whereas the remaining six stations are within a maximum distance of 90 km of its boundary. Hydro-climatic data are provided by the National Water Agency (ANA) (2020a) through the platform HIDROWEB and by the National Institute of Meteorology (INMET) (2020) through the platform BDMEP. The availability of monthly average values for the period of January 2000 to June 2019 in general was above 90%, with two exceptions. Additionally, for the stations H, K and J (located outside the map area), rainfall data was acquired for the period January 1980 to June 2019 to analyse historical drought events. The data from four streamflow gauges (ANA, 2020a) were acquired; three stations are located on the Rio Muriaé and one on the tributary Rio Carangola.

Table 1: Hydro-climatic monitoring stations and data for the period of January 2000 to June 2019
a: Station numbers with five digits are administered by INMET and those with 8 digits by ANA.
b: All stations listed were used to characterise the study region. Those not plotted in Figure 1 are located outside of the extent of the figure.

ID	Name	Source and Station code [a]	Alt. (masl)	Latitude	Longitude	Precipitation	Temperature	Humidity	Wind speed	Sunshine hours	Streamflow
A	Caparaó	83639	843	-20.52	-41.91	✓	✓		✓	✓	
B	Itaperuna	83695 / 58940000	124	-21.22	-41.90	✓	✓	✓	✓	✓	✓
C	Juiz de Fora	83692	949	-21.86	-43.46	✓		✓	✓		
D	Campos dos Goytacazes	83698	11	-21.73	-41.35	✓	✓	✓			
E	Codeiro	83718	506	-22.03	-42.46	✓	✓				
F	Viçosa	83642	712	-20.85	-42.97	✓	✓			✓	
G	Caiana	02041005	159	-20.70	-41.92	✓					
H	São Francisico do Glória	02042014	588	-20.79	-42.27	✓					
I	Porciúncula	02042027 / 58934000	823	-20.97	-42.04	✓					✓
J	Italva	02141003	59	-21.45	-41.63	✓					
K	Patrocínio de Muriaé	02142002 / 58920000	186	-21.15	-42.22	✓					✓
L	Cardoso Moreira	58960000	28	-21.50	-41.61						✓

To calibrate and validate the WEAP model, monthly means of various hydro-climatic variables are required. Values for the wind speed, precipitation and humidity were directly calculated by using two-dimensional inverse-distance-weighting interpolation (IDW) and deriving representative values for each sub-catchment.

The temperature data of the climate stations was used to derive a regression function of measured monthly temperature and the stations altitude. The raster values of the digital elevation model (DEM) were inserted in the regression function to calculate a raster layer containing the calculated temperature for each pixel.

The cloudiness factor was determined by dividing the average sunshine hours by the maximum possible sunshine hours within a month based on the latitude of the station (Allen et al., 1998).

Land use

Land use maps from 2000 and 2018 with a 300 m spatial resolution were used to quantify land use changes (ESA, 2019). The maps classify 22 land cover types following the scheme of the Food and Agricultural Organization of the United Nations (FAO). For simplification, the different land use classes were grouped. Table 2 shows that no substantial land use changes occurred in the study area over the modelled period.

Table 2: Coverage of different land use classes in the catchment for the years 2000 and 2018

Land use class	2000 in (%)	2018 in (%)
Agriculture	7.1	7.0
Sparse Forest	15.0	14.9
Forest	8.9	9.2
Grassland	68.6	68.3
Wetlands	< 0.1	< 0.1
Urban area	0.4	0.6
Water bodies	< 0.1	< 0.1

Climate change projections

As global climate models (GCMs) are too coarse to display local weather phenomena, the results of a downscaled climate model were used for this study. The Research Program on Climate Change, Agriculture and Food Security (CCAFS) (2020) provides downscaled regional projections with the 30-year mean monthly values for the time period 2020 to 2049 (referred to by CCAFS as “RCP 8.5 2030” and “RCP 2.6 2030”) and 2040 to 2069 (“RCP 8.5 2050”). These scenarios consider the expected lower (RCP 2.6) and upper (RCP 8.5) bounds of the development of worldwide greenhouse gas emissions. Mean monthly values of the climate change projections for the study area are displayed in Figure 2 and are compared to the historical data. The GCM Hadley Global Climate Model 2 (HadGEM2-ES) selected for this study was processed by the Delta Method (Navarro-Racines et al., 2020), which is a statistical downscaling method. A comparison of the HadGEM2-ES model results to other GCMs is provided in the Supplemental Material A.

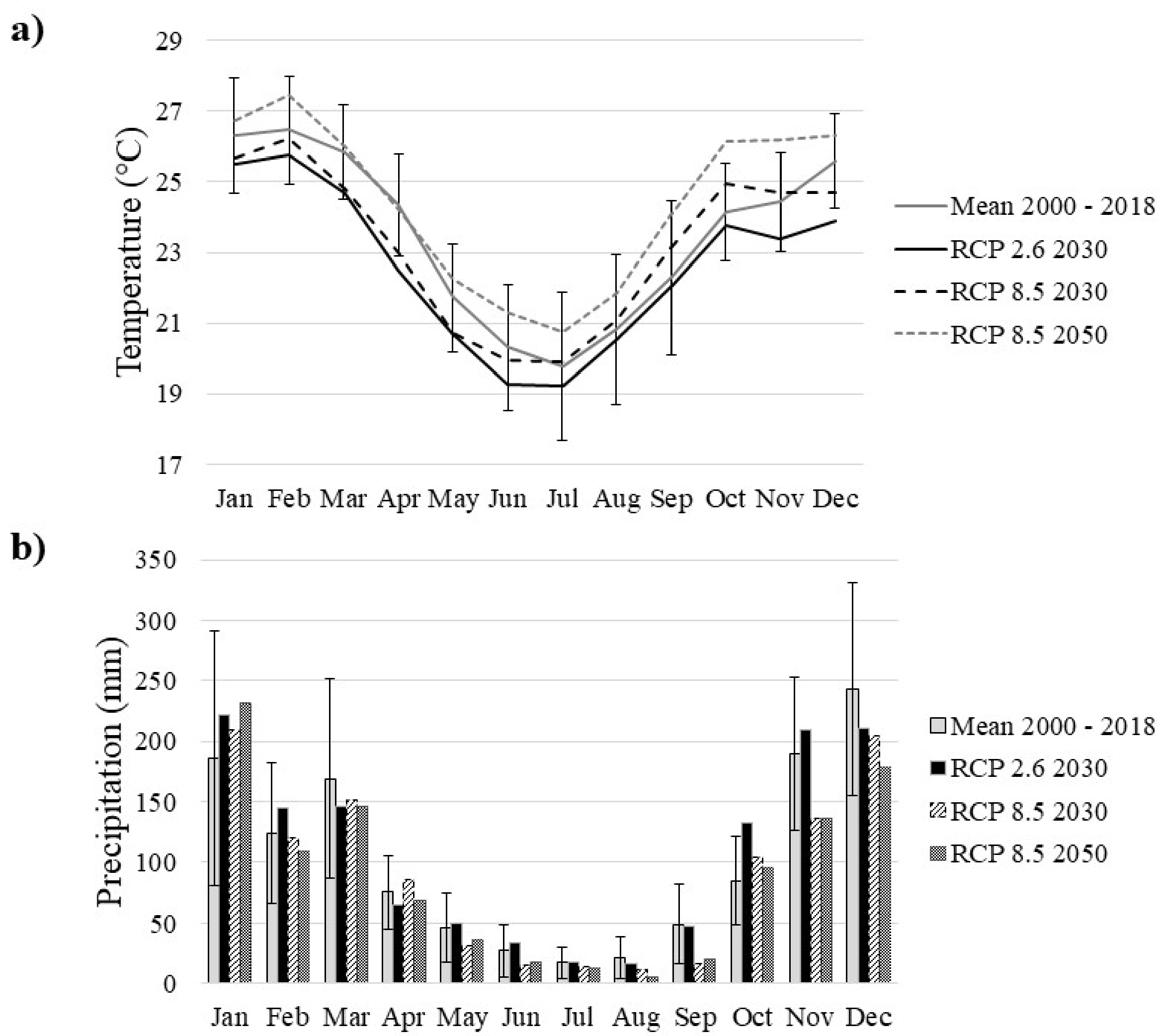

Figure 2: a) Mean monthly temperature for 2000 – 2018 and for climate projections.
b) Mean monthly precipitation for 2000 – 2018 and for climate projections. Error bars indicate one standard deviation.

Water demand and future projections

Water demand for household uses was derived from data provided by information portal SIGA by CEIVAP (2020) in combination with population data provided by the Brazilian Institute of Geography and Statistics (IBGE) (2020). Water demand for agricultural and industrial purposes was derived from water abstraction allowances published by ANA (2020a) for the two main rivers, the Muriaé River and the Carangola River. The dataset provides monthly abstraction allowances for every user and the purpose of water use. Estimates per federal state by ANA (2020b) were used to estimate the demand in the tributaries. The estimates provide annual mean abstraction rates divided into three sectors (public, industry, and agriculture) for the federal states Minas Gerais and Rio de Janeiro in the years 2012 and 2040.

ANA (2020b) only provided rough estimates for industrial and agricultural demand in the year 2040. Using a linear regression, the growth rate was applied to the historical values to estimate a trend for the years and was considered linear until 2050. Public demand growth instead was implemented following the population projections by IBGE (2020), under the assumption that demand per household remains constant.

Groundwater

Limited information is available regarding groundwater in the catchment. The general groundwater flow direction is from north-west to south-east (Prado et al., 2005), following the topography and general direction of river flow. The aquifer below the north-western area of the catchment is equally divided between heavily fractured rocks associated with the Juiz de Fora complex and the Paraíba do Sul complex, which both are metamorphosed complexes with different chemical compositions (Gonçalves et al., 2005).

2.3 Methodology

Drought assessment

We applied the widely used SPI (McKee et al., 1993) to assess meteorological drought anomalies. An advantage of the SPI is that it can characterise drought periods over user defined accumulation periods that are representative for either short term meteorological anomalies (e.g. SPI-1) or hydrological and storage related drought severity (e.g. SPI-12 and SPI-24) (Vicente-Serrano and López-Moreno, 2005), requiring only precipitation values as input data (Barker et al., 2016). The SPI-12 was calculated for three precipitation measurement stations (ID: H, J , K) for the period 1980 to June 2019, to define historical drought periods. Station H is located in the upstream mountain region, station K in the middle of the catchment and station J downstream.

Water allocation and scenario modelling - WEAP

The water allocation software tool WEAP (Water Evaluation and Planning System) (Yates et al., 2005), developed by the Stockholm Environmental Institute, is widely used for applications related to water management and scenario development to address potential climatic, socioeconomic and adaptation/response related changes (e.g. Sutton et al., 2013; Bhave et al., 2016, 2018). WEAP is a node–based, semi-distributed model that provides a user-friendly, flexible and comprehensive framework for complex water systems and can simulate monthly streamflows for each sub-catchment node in dependence of climate (rainfall-runoff module), catchment characteristics and water demand (Yates et al., 2005; Li et al., 2015).

We applied the “rainfall runoff soil moisture” approach to calibrate six sub-catchments, with the outlet of each of them corresponding to either a streamflow gauge or a potential reservoir (Figure 3). Because of the limited information on groundwater levels, only one aquifer was established to model infiltration from the river in the aquifer. Within each sub-catchment, supply and demand points were linked to the river to model water extractions and inflow.

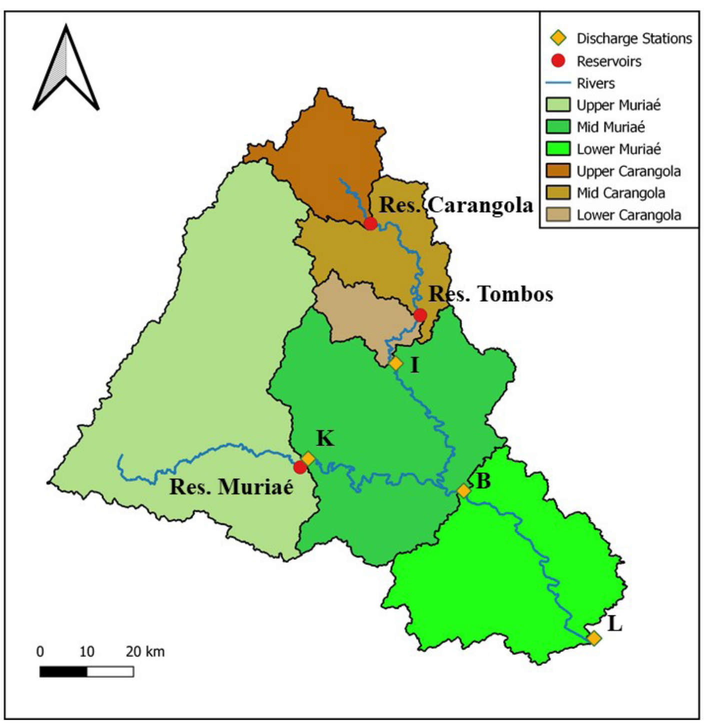

Figure 3: Visualisation of the six modelled sub-catchments, the four streamflow gauges and the location of the three potential reservoirs considered as adaptation measures in the scenarios. IDs according to Table 1.

Calibration and Validation

For the calibration and validation of each sub-catchment the monthly mean interpolated values of hydro-climatic station data (Table 1) was used. To account for the differing dominating multi-year patterns in local climate, we selected two distinct calibration periods according to wetter and drier periods (e.g. Westra et al., 2014; Thirel et al., 2015; Nauditt et al., 2017a; Gao et al., 2017). A key reason for this selection is that the catchment is characterised by a heavily fractured aquifer, which leads to a strong interdependency between groundwater levels and streamflow during drought events. The baseflow component of the streamflow can therefore be expected to decay quicker and hydrological droughts to evolve quicker than in aquifers with lower permeability (Stoelzle et al., 2014).

Sub-period calibration of wet and dry periods were defined based on the SPI-12 analysis (Figure 4a). 2000 to 2012 represents a wetter period with an average SPI-12 of 0.46, while 2013 until June 2019 represents a drought period with SPI-12 values lower than -1 (one exception), with a mean value of -0.89. Figure 4b illustrates the model warm-up period (01/2000 - 12/2001),wet period (01/2001 - 12/2013) and drought period (01/2013 until 06/2019). The wet and drought periods are then divided for calibration and validation.

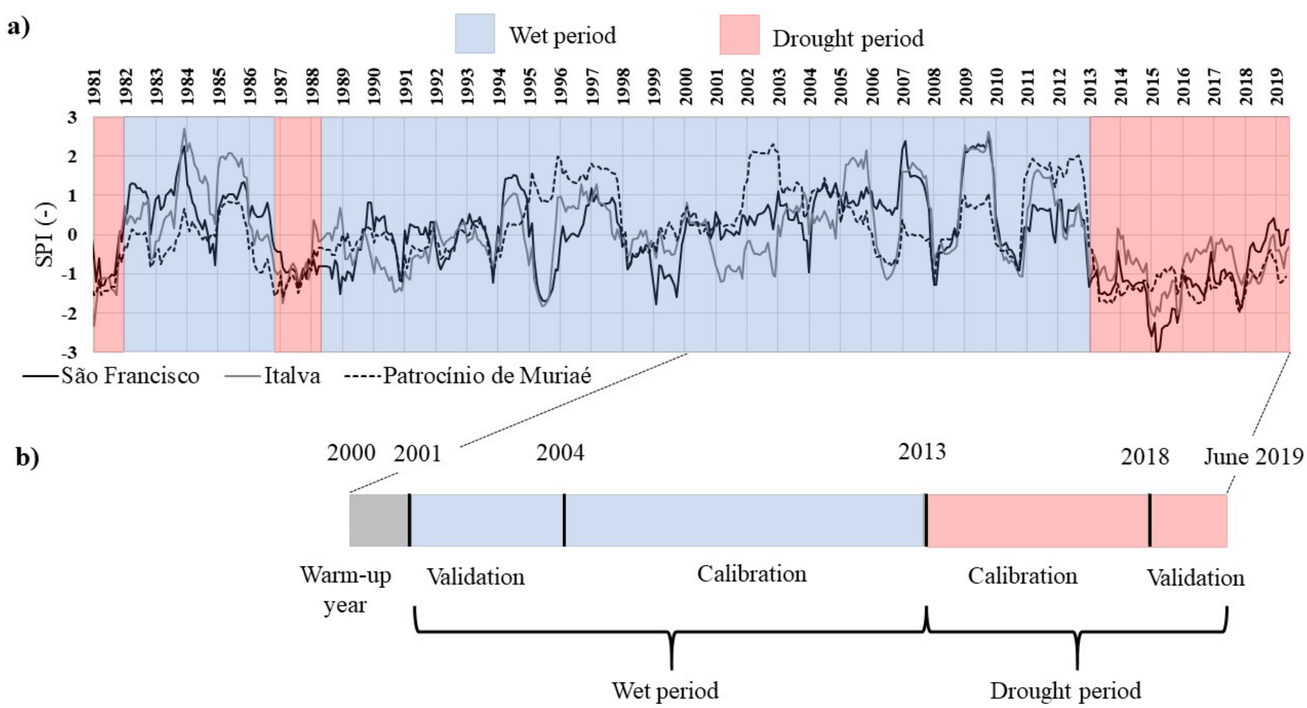

Figure 4: a) SPI-12 results for the period 1981 to 2019 with wet periods (blue) and drought periods (red) for three precipitation stations located within the study area (station codes indicated in Table 1). **b)** The results of the SPI-12 analysis were used to define the warm-up, wet and drought periods, as well as the division into calibration and validation periods, for the WEAP model.

The Parameter Estimation Tool (PEST) from the WEAP programme was used to calibrate the six sub-catchments against streamflow observations. The most relevant calibration parameters are the runoff-resistance-factor, root-zone-conductivity, soil-water-capacity and preferred-flow-direction. Furthermore, deep-zone-conductivity and initial storage of the top and bottom soil layer were adjusted. Kc values for different land use classes were adopted from results published by Allen et al. (1998) and de Oliveira et al. (2014).

Scenario development

Scenarios

To estimate water availability under potential changes, six scenarios were developed using climate change projections and drought adaptation measures, entailing reservoir construction and land use changes towards SPS (Table 3). The baseline scenarios (2.6_b and 8.5_b) only consider precipitation and temperature changes resulting from the climate change projections, without drought adaptation measures. Scenarios with the appendix "_r" consider effect of potential reservoir storage on future water availability, while the "_s" scenarios study the effects of potential land use change towards SPS Further information on the implementation of the adaptation measures is provided below.

Table 3: List of development scenarios applied in the model

Name	RCP	Adaption measures
2.6_b	2.6	None
2.6_r	2.6	Reservoirs
2.6_s	2.6	Land use change to silvopasture
8.5_b	8.5	None
8.5_r	8.5	Reservoirs
8.5_s	8.5	Land use change to silvopasture

Climate projections

Many climate change impact studies focus on the changes in mean climate, meaning that they underestimate the full impact of climate change, more specifically that of more intense droughts and floods (Thornton et al., 2014). Therefore, to adequately assess the effect of drought adaptation measures, modelled future precipitation time series and temperature time series should reflect natural climate variations. Mean monthly values for a total period of 30 years, as supplied by the climate change projections from CCAFS (2020), are considered insufficient to obtain this goal.

To include the desired climate variations, the projected precipitation and temperature time series were generated using the following steps (Figure 5):

1. Calculation of the mean monthly temperature and precipitation for the historical data (January 2000 to June 2019).
2. Calculation of the percentage deviation of the measured historical data from the historical mean value for the 15 years 2004 to 2018. This period was chosen as it covers a normal period as well as a drought period according to the SPI-12 analysis.
3. Linear interpolation between the historical mean calculated in Step (1) and the results of the climate projections.
   I. For the RCP 8.5 scenario, mean values for the 30-year period 2020 to 2049 and 2040 to 2069 were available. The data was interpolated to meet the projected values.
   II. For the RCP 2.6 scenario, only one projection (2020 to 2049) was available. The interpolation meets the projected mean value after 15 years and is then extrapolated with the same slope.
4. To include natural variations in the time series, the historic deviations calculated in Step (2) were applied to the linear interpolated values of Step (3).

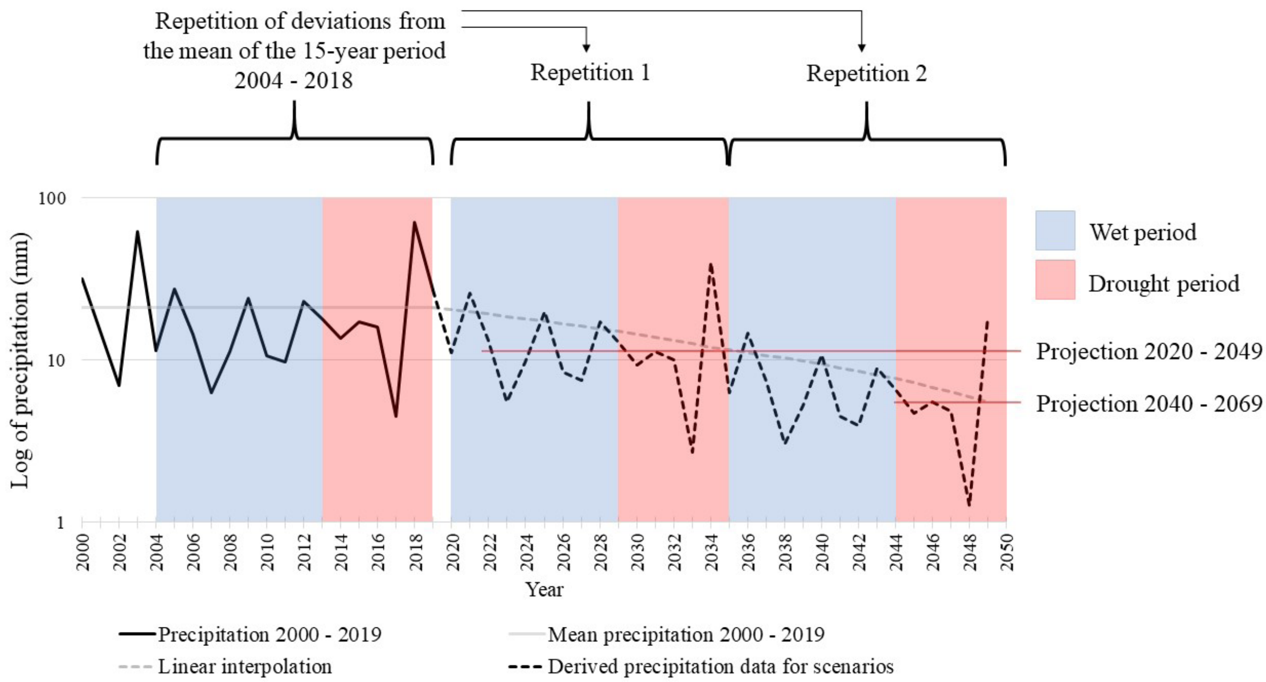

Figure 5: Example of the time series synthesis for the August precipitation values in the Upper Muriaé sub-catchment

Reservoirs as drought adaptation measure

To evaluate the effect of potential reservoir storage, we incorporated information for existing construction plans for increasing reservoir storage. The construction of three reservoirs is planned in the basin to protect the large cities against flooding (ANA, 2019). The planned locations of these reservoirs are indicated in Figure 3, with the storage capacities listed in Table 4.

Table 4: Storage capacities and location of the three reservoirs planned in the study area

Municipiality	River	Storage capacity (hm³)	Latitude	Longitude
Carangola	Rio Carangola	20.3	-20.694	-42.094
Tombos	Rio Carangola	23.1	-20.869	-41.989
Muriaé	Rio Muriaé	104.4	-21.168	-42.231

Although the primary intention of the reservoirs is to limit the flooding hazard to cities located downstream, they also have the potential to store water that can be released in order to maintain minimum levels of stream-flow downstream. To prevent a lack of water availability for public supply and agriculture during drought, the streamflow can be increased during the driest months of the year (Wanders and Wada, 2015). To ensure that the increased streamflow is available for consumers, water allocation infrastructure would be required such as distribution channels for irrigation and water supply.

WEAP does not offer an optimisation algorithm for reservoir operation. Water is only released from reservoirs in the model if there is unmet demand downstream or to satisfy designated minimum flow requirements (e.g. for ecological purposes) below the reservoir location.

The minimum flow requirement was derived by applying a flow duration curve analysis of historic streamflow from 01/2000 until 06/2019 and using a 90 percentile flow (Q90) (HR Wallingford et al., 2003). 90% of the time the observed streamflow was above 20.1 m^3/s, hence this flow requirement (for simplification, 20 m^3/s) was set at the outlet of the study area to ensure water supply for both human and environmental demands during dry months.

Silvopastoral Systems as a land use related adaptation measure

Santos et al. (2018) studied the effect of SPS in Brazil's Cerrado region, which exhibits climate conditions similar to the study area. Eucalyptus urograndis *(Eucalyptus grandis x E. urophylla)* seedlings were planted with row spacings of 12 and 22 meters. Because of the similar climate characteristics, the implementation of an equivalent SPS is considered in the scenarios developed for this study area. Four years after planting, the areas converted to SPS were considered equivalent in hydraulic parameters to sparse forest, because afforestation measures deliver desired hydrological features quickly after implementation (Ilstedt et al., 2007). The implementation rate was set to an annual increase of 2% of total grassland area available in the catchment, starting in 2025; thus, the effects on the hydrological system are modelled from the year 2029 onwards. Kc values for the Eucalyptus trees were set to 0.85 (Alves et al., 2013).

3. Results

3.1 Assessment of historical meteorological drought periods

The SPI-12 analysis reveals three meteorological drought periods over the period 1981 to 2019 (Figure 4a). The first drought period commenced before 1981, hence the complete length of the drought could not be determined. The second drought period lasted from 1987 until mid-1988. The third drought period took place from 2013 until the end of the period analysed (mid-2019), making it the longest and most intense of the three drought periods, with SPI-12 values nearing -3 for station H. During all three characterised drought periods, the SPI-12 values for the three stations exhibit similar patterns and values, indicating that the meteorological droughts developed similarly over the spatial extent of the catchment.

3.2 Estimated changes in Climate Change Projections compared to the historical mean

Table 5 shows the predicted changes in mean annual precipitation and temperature derived in the time series of the RCP 2.6 and the RCP 8.5 scenarios compared to historical values (2000 – 2018). For the RCP 2.6 scenarios, the average temperature is expected to be about 0.5 °C lower and the precipitation rate about 66 mm/a (+ 5.3%) higher than the historical period. In contrast, for the RCP 8.5 scenario, the average temperature is about 0.4 °C higher and the mean annual precipitation drops by around 85.2 mm (- 7.1%).

Table 5: Mean precipitation and mean temperature change calculated for the generated time series compared to the historical period 2000 to 2018

	Precipitation change	Temperature change
RCP 2.6	+ 66 mm/a	- 0.5 °C
RCP 8.5	- 85.2 mm/a	+ 0.4 °C

3.3 Model Calibration and Validation

Figure 6a shows scatter plots comparing the monthly observed and simulated streamflow at the four streamflow measurement stations, showing results for both the calibration and validation periods. In general, there is a strong agreement between modelled and simulated streamflow at all four streamflow gauges for both the calibration and validation periods. Table 6 lists the NSE coefficients calculated at the four streamflow stations for the calibration period and validation period for both the wet period and the drought period. For the wet period, the values for all stations are above 0.70, whereas during the drought period, the lowest value is 0.62. In general, the NSE values are higher within the wet period reaching up to 0.88 (Station L) with the exception for station I, which performs better during the drought period. The most notable discrepancies between modelled and simulated data are during the low flow months, where the simulated streamflow tends to be higher than the observed streamflow, as seen in the bottom left of the separate plots for each station. Figure 6b plots the flow hydrographs of simulated and observed streamflow at the outlet of the study area (Station L), also showing a strong agreement. The largest differences are visible during two high streamflow events observed in 2007 and 2012, where the model simulates lower values than the observed data.

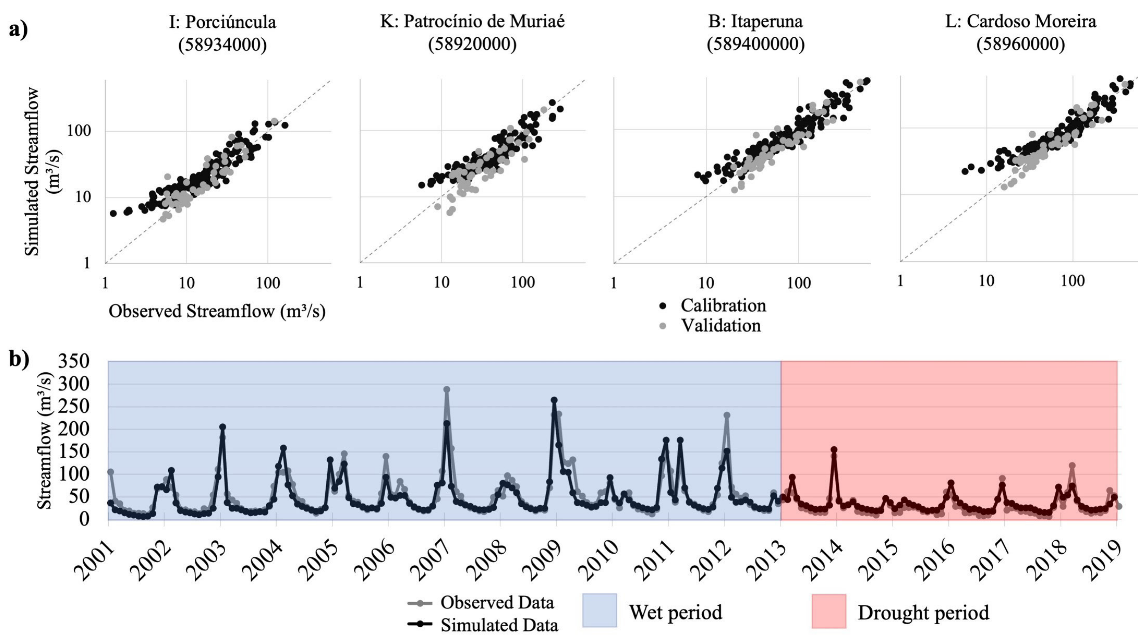

Figure 6: a) Scatter plots of observed and simulated streamflow for the four streamflow gauges. **b)** Flow hydrograph at the outlet of the modelled catchment (Station L: Cardoso Moriera), showing the observed data and simulated streamflow.

Table 6: NSE coefficient calculated at each streamflow gauge located in the study area

Streamflow gauge	Wet period		Drought period	
	Validation	Calibration	Calibration	Validation
I: Porciúncula (Lower Carangola)	0.73	0.73	0.70	0.87
K: Patronício de Muriaé (Upper Muriaé)	0.75	0.80	0.62	0.67
B: Itaperuna (Mid Muriaé)	0.87	0.82	0.67	0.65
L: Cardoso de Moreira (Lower Muriaé)	0.88	0.81	0.72	0.62

3.4 Scenario Analysis

As an increased water availability is suggested by RCP 2.6 scenarios with increased precipitation rates and lower temperature compared to the historical values, only the RCP 8.5 scenarios are evaluated to test the potential effect of the adaptation measures under drier conditions. In Table 7 the mean streamflow at the catchment outlet is displayed for the historical period and the RCP 8.5 baseline scenario (8.5_b). During all seasons, lower streamflow was simulated for the future scenario, with the percentage reduction in streamflow more pronounced over the simulated drought event 01/2044 – 12/2049. In particular simulated dry season flow (JJA) resulted in a mean reduction of 42% compared to the historical drought period.

Table 7: Mean streamflow (m3/s) at the outlet of the study area for the historical period and the RCP 8.5 baseline (8.5_b) scenario divided in 3-monthly periods.

	DJF	MAM	JJA	SON
01/2001 – 12/2018 (historical complete)	180.8	105.9	43.3	56.2
01/2013 – 12/2018 (historical drought)	87.0	60.2	26.1	33.6
01/2020 – 12/2049 (8.5_5 complete)	155.1	86.7	34.1	47.0
01/2044 – 12/2049 (8.5_b drought)	55.2	38.1	15.1	19.2

Figure 7a shows the flow hydrographs (2020 – 2050) for the three scenarios under RCP 8.5. The years 2044 to 2049 show the most severe hydrological droughts in the simulated streamflow values for the low flow months during this period and are presented in Figure 7b. With the modelled reservoir storage volume and reservoir operations (8.5_r), streamflow of 20 m3/s can be maintained at the outlet of the most downstream sub-catchment during the majority of the dry months. However, from the year 2047 onwards, the streamflow drops below 20 m^3/s at the end of winter because the reservoirs run empty after a series of dry months. While the 8.5_s (i.e. silvopasture) scenario suggests only a very minor increase in streamflow by 2.8% compared to the baseline scenario 8.5_b, the reservoir based scenario shows an increase in downstream flow by 6.4% in the low flow months from 2044 to 2049.

The land use change towards SPS resulted in a higher simulated streamflow in almost every month observed. To evaluate the effects of the land use change on the hydrological system, the monthly deviations of streamflow compared to the baseline scenarios were calculated (Figure 7c). The results show that the land use change resulted in lower streamflow in the high-precipitation months during summer, with maximum flow reduction of 4% to 8% in January and December in all sub-catchments. In the months May to October, the streamflow deviation varies between the different locations; the catchments Upper Muriaé and the three Rio Carangola catchments tend to have higher streamflow deviations with the maximum rise happening in August and September of up to +15%. In the catchments Mid Muriaé and Lower Muriaé, the maximum streamflow increase is simulated for the drier winter months June, July and August and is between +2 and +4%.

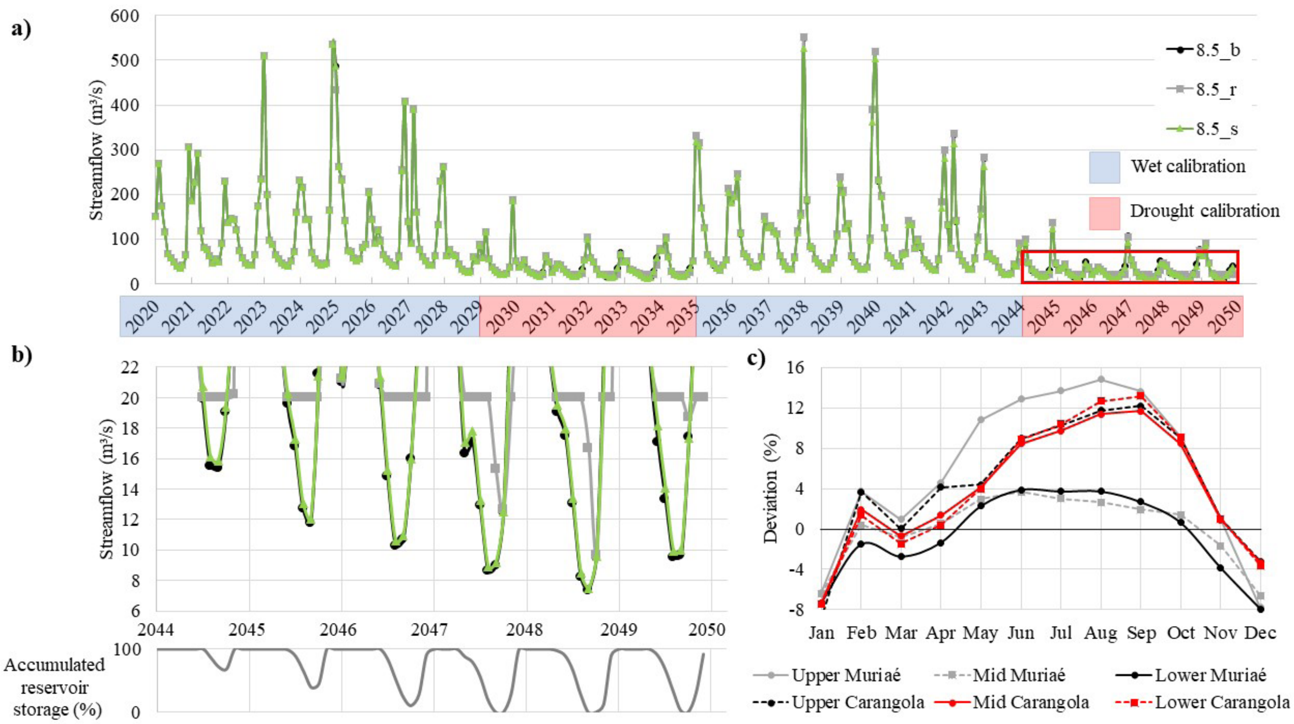

Figure 7: a) Flow hydrograph at the outlet of the study area showing the scenarios 8.5_b, 8.5_r and 8.5_s; **b)** Zoomed-in section of the area marked in 7a for the drought period 2044 to 2049 and the reservoir storage as a percentage of full capacity; **c)** Mean monthly streamflow deviation per catchment in the 8.5_s scenario compared to the 8.5_b scenario over the drought period 2044 to 2049.

4. Discussion

4.1 Model calibration and validation based on dry and wet periods

The calibration of rainfall-runoff models can be challenging in regions of strong seasonality and prone to extreme events (Gao et al., 2017). South America is additionally exposed to a strong long term climate variability with multi-year periods of consecutive dry and wet years.

A priori calibration of the entire record period resulted in poor NSE values (>0.43). As suggested by Nauditt et al. (2017a), sub-period calibration is a common approach to take into account such seasonal or even multi-year dry and wet periods. By using separate calibration periods for wet and dry periods, the adapted calibration criteria increased model performance for both periods. All NSE coefficients are within the acceptable range of >0.5 as defined by Moriasi et al. (2007) for monthly streamflow. For the wet period, the values for all stations are above 0.70 (good). During the drought period, the lowest value is 0.62 (satisfactory). Regarding the spatial performance of the model, the NSE coefficients calculated in catchments further downstream (Mid Muriaé, Lower Muriaé) show better performances, particularly during the wet period, with NSE coefficients ranging between 0.81 and 0.88.

The lower NSE values of the downstream station can be attributed to the strong immediate streamflow and baseflow response to meteorological drought due to the heavily fractured aquifer and alluvial characteristics of the downstream river bed (Nauditt et al., 2019b), meaning that reduced precipitation would lead to a quick reduction in groundwater levels. Baseflow is often considered to be the groundwater recharge component of the streamflow (Partington et al., 2012), hence it contributes a significant part of the streamflow during drought events and streamflow will show an immediate response during drought events. Future work on streamflow separation in this catchment could help improve our understanding of important aquifer-stream interactions in this basin and how they affect hydrological drought.

4.2 Scenario Development: how Climate Change might affect streamflow in the catchment

One objective of the study was to establish development scenarios for the catchment considering climate change projections. Results of a downscaled global climate model (RCP 2.6 and RCP 8.5) were incorporated into the WEAP model. These RCPs represent the lower and upper bounds of expected climate change scenarios.

Uncertainties when using climate models result from the complex dynamics of the climate system itself (response of the climate system to increases in greenhouse gas concentrations, including sensitivity and feedback processes) as well as the uncertainties associated with climate modelling for regional analysis (parameterisation, resolution and boundary conditions) (Foley, 2010). As the purpose of the incorporation of climate change projections is to provide input data to test adaptation measures under a wide range of conditions, rather than to provide actual forecasts, we assumed that the modelled scenarios adequately represent the effects of the bounding RCPs.

The mean values for monthly precipitation and temperature provided by the adopted climate change projections were compared with the historical data observed in the study area during the two calibration and validation periods (01/2001 to 06/2019). For the RCP 2.6 scenario, mean temperatures were slightly lower than the historical values. Unfortunately, downscaled results of the climate model using hindcast data were not made available by CCAFS, meaning that the forecast data could only be compared against the historical data calculated from the hydro-climatic stations.

The results of the RCP 8.5 scenarios are consistent with other studies, which suggest an increase in mean temperature and decrease in precipitation in the region (Vera et al., 2006; Marengo et al., 2012; Spinoni et al., 2020). Climate change projections with a finer temporal resolution would be required to improve the forecasting ability of the established model (Wang et al., 2009), because mean values over a thirty-year period are not sufficient to represent climate variation to test the adaptations measures in drought and wet periods.

The scenarios cover projected impacts of climate change and cover wet and drought periods, suggesting that the developed model provides valuable information to decision makers. The applied methodology can therefore be considered as a transferable approach to deliver climate change projections and hence a baseline to analyse the effects of various adaptation measures in terms of available water throughout a river basin.

4.3 Effect of Potential Adaptation Measures on Water Availability

Increase of reservoir storage

During the drought of 2014/2015, municipalities in the catchments declared a state of emergency and experienced drought damages in agriculture (Prefeitura do Município de Italva, 2017; Prefeitura Municipal de Itaperuna, 2017). However, the results of the baseline scenario modelling show that a combination of comparable drought events under climate change and substantial growth in water demands still results in no unmet demand. This suggests that water was available in the main river system, but the catchment lacks a distribution system to supply water to where it is needed or that unmet demand occurred on a time scale smaller than the monthly time step that we modelled. In tropical catchments, just a few days without rain can lead to water deficits that affect livestock and rain-fed agricultural production (Nauditt et al., 2020).

A drought risk map published for the catchment indicates that the highest drought risk is present in the meteorologically drier downstream area, where most economic activities are concentrated (Nauditt et al., 2020). The introduction of reservoirs has the potential to significantly increase streamflow during the dry months and provide downstream water supply. In the scenarios with modelled reservoirs, the summer precipitation was sufficient to refill the reservoirs every year. Only the extended dry period from 2047 to 2049 resulted in streamflow values at the catchment outlet below 20 m³/s in the end of winter because the reservoirs run empty and are unable to provide enough water to maintain this designated minimum flow requirement. Modelling reservoir operations to serve both flood protection and that of drought adaptation management is not possible in WEAP. Such operations require ensuring sufficient refill in the wet months and maintaining free volume for water retention in the wet season, the latter of which should involve an analysis at either the daily or hourly temporal scale. The definition of optimal operation rules for multi-purpose reservoirs aiming to maximise utilisation under the condition of flood control has been subject of ongoing research (e.g. Liu et al., 2011; Anand et al., 2018) and is outside the scope of this work.

Silvopastoral measures

According to Bruijnzeel (2004), no-well documented cases exist where afforestation measures produced a corresponding increase in streamflow. Compared to the planned reservoirs, the modelled widespread implementation of SPS appears to have marginal effects on coping with drought for users downstream of the reservoirs. In the SPS scenarios, the converted areas are associated with a higher Kc value compared to the grassland areas, which in general results in higher evapotranspiration. The applied model in this study does not provide direct information on evapotranspiration and baseflow, but the simulated land use changes do not result in lower streamflow than in the baseline scenario during low-flow periods and thereby do not worsen the drought propagation in the catchment. The conceptual model character of WEAP does not distinguish between the relevant processes resulting in higher streamflow despite reduced evapotranspiration.

Multiple studies have demonstrated that afforestation measures can attenuate streamflow peaks (Bhave et al., 2016; Bhattacharjee and Behera, 2017; Johnen et al., 2020), as was reflected in the outputs of the WEAP model. An intensified effect can be observed in the upstream catchments characterised by higher topography and slopes compared to the downstream catchments. Conversely, the implementation of SPS increased streamflow in all modelled catchments during the dry winter months, when the drought risk is the highest. Our results support the hypothesis that land-use changes have relatively little effect on the overall water yield but can modify streamflow in terms of timing and magnitude during extremes (Birkel et al., 2012), and suggest that SPS can increase water availability for streamflow abstractions and provide a valuable service against the depletion of water resources. Further positive effects of the implementation of SPS are the reduction of soil degradation and erosion (de Aguiar et al., 2010). In particular, reduced erosion would be a beneficial effect because it decreases sedimentation load reaching the reservoirs (Schleiss et al., 2016) in the event that both adaptation measures were to be adopted. Furthermore, SPS work as a decentralised solution compared to the centralised solutions offered by reservoirs.
No large catchment-scale implementation of SPS was conducted so far in Brazil. Determining factors in the potential success of a potential widely applied introduction would be the level of response from farmers and the considerations of costs of implementation and labour (Fischer et al., 2018).

5. Conclusion

The historic drought in 2014/2015 and the accompanying damage have shown that the Muriaé catchment in South-east Brazil requires appropriate plans for drought adaptation. Considering climate change projections and socio-economic development projected for the study area, an increased risk of drought can be expected in the future.

A WEAP model at the monthly temporal scale was established to evaluate the water supply potential of adaptation measures. The model, which was calibrated using two sub-periods, sufficiently manages to reproduce the historical measured streamflow data and therefore was considered suitable to obtain reliable results for a scenario analysis. In total, six scenarios were modelled, with climate projections based on RCP 2.6 and RCP 8.5 for the HadGEM2-ES GCM, representing the lower and upper bound of greenhouse gas emission projections, and adaptation measures based on reservoir construction and land-use change towards SPS as the input variables. During no time step was unmet demand simulated for any of the six development scenarios. An adaptation based on reservoirs has the potential to almost always maintain the required streamflow for ecological purposes (20 m^3/s) in the low-flow months during drought events. In comparison, the land use change towards SPS only led to minimal increase of a maximum of 4% in the low-flow period.

For the stakeholders in the catchment, the planned reservoirs in the catchment could have beneficial effects on the water availability in the catchment during droughts, but sufficient infrastructure would be required to make this water available in the locations where it is needed. Further research is required to derive optimal reservoir operation to ensure that both the purposes of flood protection and drought adaptation can be simultaneously met. SPS can be considered a “no-regret” option for nature-based drought adaptation, particularly because it functions as a decentralised measure, and can be implemented in addition to reservoir construction. The additional benefits of SPS would be limited erosion and sedimentation of the newly established reservoirs, and also increased streamflow during drought periods.

The established methodology is a valuable approach as a first assessment of the effect of adaptation measures on streamflow in this data-scarce catchment.

6. References

Alamanos, A., Latinopoulos, D., Papaioannou, G., Mylopoulos, N., 2019. Integrated Hydro-Economic Modeling for Sustainable Water Resources Management in Data-Scarce Areas: The Case of Lake Karla Watershed in Greece. Water Resour Manage 33, 2775–2790. https://doi.org/10.1007/s11269-019-02241-8

Allen, R.G., Pereira, L.S., Raes, D., Smith, M., 1998. FAO Irrigation and drainage paper No. 56. Food and Agricultural Organisation of the United Nations, Rome.

Alves, M.E.B., Mantovani, E.C., Sediyama, G.C., Neves, J.C.L., 2013. Estimate of the crop coefficient for Eucalyptus cultivated under irrigation during initial growth. CERNE 19, 247–253. https://doi.org/10.1590/S0104-77602013000200008

ANA Agência Nacional de Águas, 2020a. HIDROWEB [WWW Document]. URL http://www.snirh.gov.br/hidroweb/serieshistoricas (accessed 1.9.20).

ANA Agência Nacional de Águas, 2020b. Dados de Referência [WWW Document]. URL https://www.ana.gov.br/sala-de-situacao/paraiba-do-sul/documentos-relacionados/dados- de-referencia (accessed 1.9.20).

ANA Agência Nacional de Águas, 2019. Plano Nacional de Segurança Hídrica. Ministério Do Desevolvimento Regional, Brasília.

Anand, J., Gosain, A.K., Khosa, R., 2018. Optimisation of Multipurpose Reservoir Operation by Coupling Soil and Water Assessment Tool (SWAT) and Genetic Algorithm for Optimal Operating Policy (Case Study: Ganga River Basin). Sustainability 10, 1660. https://doi.org/10.3390/su10051660

Avila-Diaz, A., Benezoli, V., Justino, F., Torres, R., Wilson, A., 2020. Assessing current and future trends of climate extremes across Brazil based on reanalyses and earth system model projections. Clim Dyn 55, 1403–1426. https://doi.org/10.1007/s00382-020-05333-z

Barker, L.J., Hannaford, J., Chiverton, A., Svensson, C., 2016. From meteorological to hydrological drought using standardised indicators. Hydrology and Earth System Sciences 20, 2483–2505. https://doi.org/10.5194/hess-20-2483-2016

Benegas, L., Ilstedt, U., Roupsard, O., Jones, J., Malmer, A., 2014. Effects of trees on infiltrability and preferential flow in two contrasting agroecosystems in Central America. Agriculture, Ecosystems & Environment 183, 185–196. https://doi.org/10.1016/j.agee.2013.10.027

Bhattacharjee, K., Behera, B., 2017. Forest cover change and flood hazards in India. Land Use Policy 67, 436–448. https://doi.org/10.1016/j.landusepol.2017.06.013

Bhave, A.G., Conway, D., Dessai, S., Stainforth, D.A., 2018. Water Resource Planning Under Future Climate and Socioeconomic Uncertainty in the Cauvery River Basin in Karnataka, India. Water Resour. Res. 54, 708–728. https://doi.org/10.1002/2017WR020970

Bhave, A.G., Mittal, N., Mishra, A., Raghuwanshi, N.S., 2016. Integrated Assessment of no-Regret Climate Change Adaptation Options for Reservoir Catchment and Command Areas. Water Resour Manage 30, 1001–1018. https://doi.org/10.1007/s11269-015-1207-4

Birkel, C., Soulsby, C., Tetzlaff, D., 2012. Modelling the impacts of land-cover change on streamflow dynamics of a tropical rainforest headwater catchment. Hydrological Sciences Journal 57, 1543–1561. https://doi.org/10.1080/02626667.2012.728707

Bruijnzeel, L.A., 2004. Hydrological functions of tropical forests: not seeing the soil for the trees? Agriculture, Ecosystems & Environment 104, 185–228. https://doi.org/10.1016/j.agee.2004.01.015

Carvalho, C.E.V.D., Torres, J., 2002. The ecohydrology of the Paraíba do Sul River, Southeast Brazil. IAHS Special Publication 6.

CEIVAP Comitê de Integração da Bacia Hidrográfica do Rio Paraíba do Sul, 2020. Sistema de Informações Geográficas e Geoambientais Da Bacia Hidrográfica Do Rio Paraíba Do Sul [WWW Document]. URL http://sigaceivap.org.br/ (accessed 1.9.20).

Chebet, C., Kipkorir, E.C., Odenyo, V.A.O., 2019. Assessment of water demand dynamics in Arror watershed in Elgeyo Marakwet County, Kenya. Journal of Water and Climate Change 10, 642–657. https://doi.org/10.2166/wcc.2018.126

de Aguiar, M.I., Maia, S.M.F., Xavier, F.A. da S., de Sá Mendonça, E., Filho, J.A.A., de Oliveira, T.S., 2010. Sediment, nutrient and water losses by water erosion under agroforestry systems in the semi-arid region in northeastern Brazil. Agroforest Syst 79, 277–289. https://doi.org/10.1007/s10457-010-9310-2 de Oliveira, C.C., Villela, S.D.J., de Almeida, R.G., Alves, F.V., Behling-Neto, A., Martins, P.G.M. de A., 2014. Performance of Nellore heifers, forage mass, and structural and nutritional characteristics of Brachiaria brizantha grass in integrated production systems. Trop Anim Health Prod 46, 167–172. https://doi.org/10.1007/s11250-013-0469-1

Dias-Filho, M.B., 2014. Diagnóstico das Pastagens no Brasil. EMBRAPA 38.

Erfanian, A., Wang, G., Fomenko, L., 2017. Unprecedented drought over tropical South America in 2016: significantly under-predicted by tropical SST. Sci Rep 7, 5811. https://doi.org/10.1038/s41598-017-05373-2

ESA European Space Agency, 2019. ESA Climate Change Initiative - Land Cover Data [WWW Document]. URL https://cds.climate.copernicus.eu/cdsapp#!/dataset/satellite-land-cover?tab=form (accessed 4.8.20).

Fischer, S., Pedraza-Luengas, A., Schlüter, S., Olivera Antunes, L., 2018. From design to implementation: a participatory appraisal for silvopastoral systems, in: Nehren, U. (Ed.), Strategies and Tools for a Sustainable Rural Rio de Janeiro, Springer Series on Environmental Management. Springer International Publishing, Cham.

Foley, A.M., 2010. Uncertainty in regional climate modelling: A review. Progress in Physical Geography: Earth and Environment 34, 647–670. https://doi.org/10.1177/0309133310375654

Fowler, H.J., Blenkinsop, S., Tebaldi, C., 2007. Linking climate change modelling to impacts studies: recent advances in downscaling techniques for hydrological modelling. International Journal of Climatology 27, 1547–1578. https://doi.org/10.1002/joc.1556

Gao, J., Christensen, P., Li, W., 2017. Application of the WEAP model in strategic environmental assessment: Experiences from a case study in an arid/semi-arid area in China. Journal of Environmental Management 198, 363–371. https://doi.org/10.1016/j.jenvman.2017.04.068

Gonçalves, J.A.C., Scudino, P.C.B., Sobreira, F.G., 2005. Reservas renováveis e caracterização dos aqüíferos fissurais do Leste da Zona da Mata de Minas Gerais e adjacências. Geol. USP, Sér. cient. 5, 19–27. https://doi.org/10.5327/S1519-874X2005000100002

HR Wallingford, University of Zimbabwe, University of Zambia, University of Zululand, Department for Water Development Ministry of Rural Resources and Water Development, Zimbabwe, 2003. Handbook for the Assessment of Catchment Water Demand and Use. HR Wallingford, Wallingford, UK.

IBGE Instituto Brasileiro de Geografia e Estatística, 2020. Population Projections 2010 - 2060 [WWW Document]. URL https://www.ibge.gov.br/en/statistics/social/population/18176-population- projection.html?=&t=downloads (accessed 1.9.20).

Ilstedt, U., Bargués Tobella, A., Bazié, H.R., Bayala, J., Verbeeten, E., Nyberg, G., Sanou, J., Benegas, L., Murdiyarso, D., Laudon, H., Sheil, D., Malmer, A., 2016. Intermediate tree cover can maximize groundwater recharge in the seasonally dry tropics. Sci Rep 6, 21930. https://doi.org/10.1038/srep21930

Ilstedt, U., Malmer, A., Verbeeten, E., Murdiyarso, D., 2007. The effect of afforestation on water infiltration in the tropics: A systematic review and meta-analysis. Forest Ecology and Management 251, 45–51. https://doi.org/10.1016/j.foreco.2007.06.014

IMNET National Institue of Meteorology, 2020. BDMEP Banco de Dados Meteorológicos Para Ensino e Pesquisa [WWW Document]. URL http://www.inmet.gov.br/portal/index.php?r=bdmep/bdmep (accessed 1.9.20).

Johnen, G., Sapač, K., Rusjan, S., Zupanc, V., Vidmar, A., Bezak, N., 2020. Modelling and Evaluation of the Effect of Afforestation on the Runoff Generation Within the Glinščica River Catchment (Central Slovenia), in: The Handbook of Environmental Chemistry. Springer, Berlin, Heidelberg, pp. 1–17. https://doi.org/10.1007/698_2020_649

Keesstra, S., Nunes, J., Novara, A., Finger, D., Avelar, D., Kalantari, Z., Cerdà, A., 2018. The superior effect of nature based solutions in land management for enhancing ecosystem services. Science of The Total Environment 610–611, 997–1009. https://doi.org/10.1016/j.scitotenv.2017.08.077

Le Breton, R., 2000. Land Management and Sustainable Development in the Atlantic Rainforest of Brazil: The Iracambi Experience. Presented at the 5th International Symposium on Environmental Geotechnology and Global Sustainable Development, Belo Horizonte.

Li, X., Zhao, Y., Shi, C., Sha, J., Wang, Z.-L., Wang, Y., 2015. Application of Water Evaluation and Planning (WEAP) model for water resources management strategy estimation in coastal Binhai New Area, China. Ocean & Coastal Management 106, 97–109. https://doi.org/10.1016/j.ocecoaman.2015.01.016

Liu, X., Guo, S., Liu, P., Chen, L., Li, X., 2011. Deriving Optimal Refill Rules for Multi-Purpose Reservoir Operation. Water Resour Manage 25, 431–448. https://doi.org/10.1007/s11269-010-9707-8

Lyra, A., Tavares, P., Chou, S.C., Sueiro, G., Dereczynski, C., Sondermann, M., Silva, A., Marengo, J., Giarolla, A., 2018. Climate change projections over three metropolitan regions in Southeast Brazil using the non-hydrostatic Eta regional climate model at 5-km resolution. Theor Appl Climatol 132, 663–682. https://doi.org/10.1007/s00704-017-2067-z

Maia, R., Vivas, E., Serralheiro, R., de Carvalho, M., 2015. Socioeconomic Evaluation of Drought Effects. Main Principles and Application to Guadiana and Algarve Case Studies. Water Resour Manage 29, 575–588. https://doi.org/10.1007/s11269-014-0883-9

Marengo, J.A., Chou, S.C., Kay, G., Alves, L.M., Pesquero, J.F., Soares, W.R., Santos, D.C., Lyra, A.A., Sueiro, G., Betts, R., Chagas, D.J., Gomes, J.L., Bustamante, J.F., Tavares, P., 2012. Development of regional future climate change scenarios in South America using the Eta CPTEC/HadCM3 climate change projections: climatology and regional analyses for the Amazon, São Francisco and the Paraná River basins. Clim Dyn 38, 1829–1848. https://doi.org/10.1007/s00382-011-1155-5

McKee, T.B., Doesken, N.J., Kleist, J., 1993. The relationship of drought frequency and duration of time scales. Presented at the Eighth Conference on Applied Climatology, American Meteorological Society, Anaheim, p. 6.

McNamara, I., Nauditt, A., Zambrano-Bigiarini, M., Ribbe, L., Hann, H., 2020. Modelling water resources for planning irrigation development in drought-prone southern Chile. International Journal of Water Resources Development 37, Issue 5, 1–26. https://doi.org/10.1080/07900627.2020.1768828

Moriasi D.N.,Arnold, J.G., Van Liew, M.W., Binger, R.L., Harmel, R.D., Veith, T.L. 2007. Model evaluation guidelines for systematic quantification of accuracy in watershed simulation. Transactions of the ASABE 50, Issue 3, 885-900. https://doi.org/10.13031/2013.23153

Nahed-Toral, J., Valdivieso-Pérez, A., Aguilar-Jiménez, R., Cámara-Cordova, J., Grande-Cano, D., 2013. Silvopastoral systems with traditional management in southeastern Mexico: a prototype of livestock agroforestry for cleaner production. Journal of Cleaner Production 57, 266–279. https://doi.org/10.1016/j.jclepro.2013.06.020

Nauditt, A., Birkel, C., Soulsby, C., Ribbe, L., 2017a. Conceptual modelling to assess the influence of hydro-climatic variability on runoff processes in data scarce semi-arid Andean catchments. Hydrological Sciences Journal 62, 515–532. https://doi.org/10.1080/02626667.2016.1240870

Nauditt, A., Firoz, A.B.M., Trinh, V.Q., Fink, M., Stolpe, H., Ribbe, L., 2017b. Hydrological Drought Risk Assessment in an Anthropogenically Impacted Tropical Catchment, Central Vietnam, in: Nauditt, A., Ribbe, L. (Eds.), Land Use and Climate Change Interactions in Central Vietnam, Water Resources Development and Management. Springer Singapore, Singapore, pp. 223–239. https://doi.org/10.1007/978-981-10-2624-9_14

Nauditt, A., Hann, H., Formiga, R., Ribbe, L., 2019a. Avaliação do risco de seca em uma bacia hidrográfica rural com escassez de dados: o caso da sub-bacia do rio Muriaé, in: Filho, F. (Ed.), Adapta Gestão Adaptativa Do Risco Climático de Seca, UFC Book Series.

Nauditt, A., Metzke, D., Thurner, R., Ribbe, L., Formiga, R., 2019b. A grande seca de 2014-2015 Na Bacia Do Rio Paraíba Do Sul: Compreendendo As Características Espaciais E Temporais De Seca E Escassez Hídrica, in: Filho, F. (Ed.), Adapta Gestão Adaptativa Do Risco Climático de Seca, UFC Book Series.

Nauditt, A., Stahl, K., Rodriguez, E., Birkel, C., Formiga-J, R.M., Marko, K., Hamish, H., Ribbe, L., Baez-Villanueva, O.M., Thurner, J., 2020. Tropical drought risk: estimates combining gridded vulnerability and hazard data. Natural Hazards and Earth System Sciences. https://doi.org/10.5194/nhess-2020-360

Navarro-Racines, C., Tarapues, J., Thornton, P., Jarvis, A., Ramirez-Villegas, J., 2020. High-resolution and bias-corrected CMIP5 projections for climate change impact assessments. Sci Data 7, 7. https://doi.org/10.1038/s41597-019-0343-8

Ortiz, R., 2012. Climate Change and Agricultural Production (No. Technical Notes IDB-TN 383). Inter-American Development Bank.

Partington, D., Brunner, P., Simmons, C.T., Werner, A.D., Therrien, R., Maier, H.R., Dandy, G.C., 2012. Evaluation of outputs from automated baseflow separation methods against simulated baseflow from a physically based, surface water-groundwater flow model. Journal of Hydrology 458–459, 28–39. https://doi.org/10.1016/j.jhydrol.2012.06.029

Peel, M.C., Finlayson, B.L., Mcmahon, T.A., 2007. Updated world map of the Köppen-Geiger climate classification 36.

Prado, R.B., Dantas, M.E., Fidalgo, E.C.C., Gonçalves, A.O., 2005. Diagnóstico do Meio Físico da Bacia Hidrográfica do Rio Muriaé. Embrapa Solos Documentos 83, 75.

Prefeitura do Município de Italva, 2017. Decreto No. 2320.

Prefeitura Municipal de Itaperuna, 2017. Decreto No. 5774.

Research Program on Climate Change, Agriculture, and Food Security, 2020. Spatial Downscaling Data [WWW Document]. URL http://www.ccafs-climate.org/data_spatial_downscaling (accessed 1.9.20).

Santos, D. de C., Guimarães Júnior, R., Vilela, L., Maciel, G.A., França, A.F. de S., 2018. Implementation of silvopastoral systems in Brazil with Eucalyptus urograndis and Brachiaria brizantha: Productivity of forage and an exploratory test of the animal response. Agriculture, Ecosystems & Environment 266, 174–180. https://doi.org/10.1016/j.agee.2018.07.017

Schleiss, A.J., Franca, M.J., Juez, C., Cesare, G.D., 2016. Reservoir sedimentation. Journal of Hydraulic Research 54, 595–614. https://doi.org/10.1080/00221686.2016.1225320

Spinoni, J., Barbosa, P., Bucchignani, E., Cassano, J., Cavazos, T., Christensen, J.H., Christensen, O.B., Coppola, E., Evans, J., Geyer, B., Giorgi, F., Hadjinicolaou, P., Jacob, D., Katzfey, J., Koenigk, T., Laprise, R., Lennard, C.J., Kurnaz, M.L., Li, D., Llopart, M., McCormick, N., Naumann, G., Nikulin, G., Ozturk, T., Panitz, H.-J., Porfirio da Rocha, R., Rockel, B., Solman, S.A., Syktus, J., Tangang, F., Teichmann, C., Vautard, R., Vogt, J.V., Winger, K., Zittis, G., Dosio, A., 2020. Future Global Meteorological Drought Hot Spots: A Study Based on CORDEX Data. Journal of Climate 33, 3635–3661. https://doi.org/10.1175/JCLI-D-19-0084.1

Sridharan, V., Pereira Ramos, E., Zepeda, E., Boehlert, B., Shivakumar, A., Taliotis, C., Howells, M., 2019. The Impact of Climate Change on Crop Production in Uganda—An Integrated Systems Assessment with Water and Energy Implications. Water 11, 1805. https://doi.org/10.3390/w11091805

Stoelzle, M., Stahl, K., Morhard, A., Weiler, M., 2014. Streamflow sensitivity to drought scenarios in catchments with different geology: STREAMFLOW SENSITIVITY TO DROUGHT. Geophys. Res. Lett. 41, 6174–6183. https://doi.org/10.1002/2014GL061344

Sutton, W.R., Srivastava, J.P., Neumann, J.E., Strzepek, K., Boehlert, B., 2013. Reducing the Vulnerability of Moldova's Agricultural Systems to Climate Change: Impact Assessment and Adaptation Options. The World Bank. https://doi.org/10.1596/978-1-4648-0045-0

Thirel, G., Andréassian, V., Perrin, C., 2015. On the need to test hydrological models under changing conditions. Hydrological Sciences Journal 60, 1165–1173. https://doi.org/10.1080/02626667.2015.1050027

Thornton, P.K., Ericksen, P.J., Herrero, M., Challinor, A.J., 2014. Climate variability and vulnerability to climate change: a review. Glob Change Biol 20, 3313–3328. https://doi.org/10.1111/gcb.12581

Trenberth, K.E., Dai, A., van der Schrier, G., Jones, P.D., Barichivich, J., Briffa, K.R., Sheffield, J., 2014. Global warming and changes in drought. Nature Climate Change 4, 17–22. https://doi.org/10.1038/nclimate2067

UNDP United Nations Development Project, 2011. Mainstreaming Drought Risk Management - A Primer. United Nations Development Programme Drylands Development Centre, Nairobi.

Unesco, World Water Assessment Programme, 2018. Nature-based solutions for water.

UN-ISDR, 2009. Drought Risk Reduction Framework and Practices - Contributing to the Implementation of the Hyogo Framework for Action. Geneva.

UN-ISDR, 2005. Hyogo Framework for Action 2005 - 2015. Geneva.

Vera, C., Silvestri, G., Liebmann, B., González, P., 2006. Climate change scenarios for seasonal precipitation in South America from IPCC-AR4 models. Geophys. Res. Lett. 33, L13707. https://doi.org/10.1029/2006GL025759

Vicente-Serrano, S.M., López-Moreno, J.I., 2005. Hydrological response to different time scales of climatological drought: an evaluation of the Standardized Precipitation Index in a mountainous Mediterranean basin. Hydrology and Earth System Sciences 9, 523–533. https://doi.org/10.5194/hess-9-523-2005

Wanders, N., Wada, Y., 2015. Human and climate impacts on the 21st century hydrological drought. Journal of Hydrology, Drought processes, modeling, and mitigation 526, 208–220. https://doi.org/10.1016/j.jhydrol.2014.10.047

Wang, Y., He, B., Takase, K., 2009. Effects of temporal resolution on hydrological model parameters and its impact on prediction of river discharge / Effets de la résolution temporelle sur les paramètres d'un modèle hydrologique et impact sur la prévision de l'écoulement en rivière. Hydrological Sciences Journal 54, 886–898. https://doi.org/10.1623/hysj.54.5.886

Westra, S., Thyer, M., Leonard, M., Kavetski, D., Lambert, M., 2014. A strategy for diagnosing and interpreting hydrological model nonstationarity. Water Resources Research 50, 5090–5113. https://doi.org/10.1002/2013WR014719

Yates, D., Sieber, J., Purkey, D., Huber-Lee, A., 2005. WEAP21—A Demand-, Priority-, and Preference-Driven Water Planning Model: Part 1: Model Characteristics. Water International 30, 487–500. https://doi.org/10.1080/02508060508691893

Supplemental Material A

Figure A1 shows the downscaled results for different GCMs (five for RCP 2.6 and seven for RCP 8.5) provided by CCAFS for South East Brazil. For the RCP 2.6 scenario no downscaled results were provided for the 2050 time period. Looking at precipitation, the results for RCP 2.6 of HadGEM-2-ES provide the second lowest data point while for the RCP 8.5 values build the median of the ensemble. Whereas for temperature, the HadGEM-2-ES model results are found at the upper bound of the ensemble for both, RCP 2.6 and 8.5.

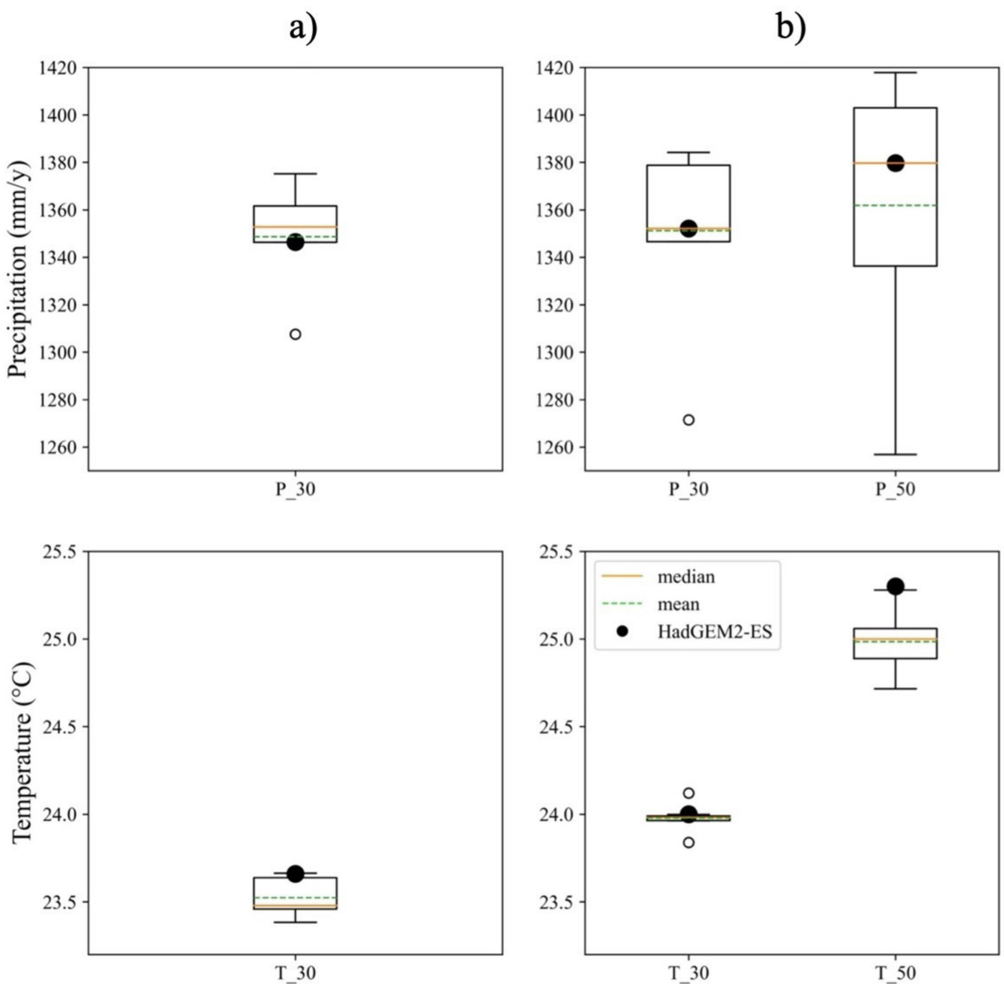

Figure A1: Boxplots indicating the range of results of an ensemble of different climate models downscaled by the CCAFS.
Column a): Ensemble for RCP 2.6 (CESM1-CAM5, MIROC-ESM, HadGEM2-ES, MPI-ESM-MR, NCAR-CCSM4) –
Column b): Ensemble for RCP 8.5 (CESM1-CAM5, MIROC-ESM, HadGEM2-ES, MPI-ESM-MR, NCAR-CCSM4, IPSL-CM5B-LR, HadG-EM2-CC). The results show the mean values over all of south-east South America (labeled as C3 area by CCAFS) for the 2030 period (P30, T30) and 2050 period (P50, T50). The model HadGEM2-ES used in this study is marked with black dots.